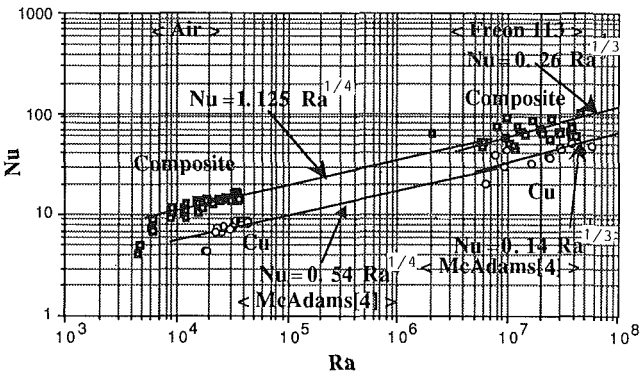

Fig. 2 Correlation of natural convection data

Test data are correlated in Fig. 2 in the form of a Nu versus Ra graph with the diameter of the heating surface as the characteristic length. Included for comparison are the empirical formulas recommended by McAdams (1955) for a heated horizontal plate facing upward. Fixing the exponents based on the McAdams recommendations, one finds the coefficients that best fit the data of the composite surface. This yields:

$$\left.\begin{aligned} &\mathrm{Nu} = 1.125\ \mathrm{Ra}^{1/4} \quad \text{for } 10^4 \le \mathrm{Ra} \le 5\times 10^5 \text{ (laminar flow)} \\ &\mathrm{Nu} = 0.264\ \mathrm{Ra}^{1/3} \quad \text{for } 5\times 10^6 \le \mathrm{Ra} \le 10^{11} \text{ (turbulent flow)} \end{aligned}\right\} \tag{2}$$

The higher heat transfer performance of the composite surface can be explained as follows: For the same temperature drop over the same thickness, the heat flux through the composite material (in the fiber direction) will be 3 to 4 times higher than through pure copper because the thermal conductivity of the composite is 3 to 4 times higher than that of pure copper. Therefore, a higher heat flux is transferred to the ambient from the composite surface than from a pure copper surface.

It is important to note that the evaporation of Freon 113 during experiments caused data scattering, especially at higher heating surface temperatures (at higher Ra). In contrast, data scattering in the case of air is minimal in the absence of phase change. The uncertainty estimations are evaluated by the method of Kline and McClintack (1953). The uncertainty intervals are ± 10 percent for air and ± 15 percent for Freon 113, since at high heat fluxes, the temperature differences in the Gr-Cu composite become very small. The sharp drop in Nu at Ra of approximately 10^4 in Fig. 2 suggests the lower limit of validity of the correlation formulas.

4 Conclusion

The reproducibility of test data for natural convection on the copper-graphite composite with a 25-mm dia heated surface facing upward is good. This is especially true in the case of air, where data scattering is much less than in Freon 113. It is revealed from this study that natural convection heat transfer on the composite surface is about two times higher than that of a pure copper surface, in both the laminar and turbulent regions. A substantial enhancement was also observed in the case of pool boiling in a previous study (Yang et al., 1991).

This work was supported by the Natural Science Foundation under Grant No. CBT-8811065.

References

Chu, R. C., and Simmons, R. E., 1988, "Heat Transfer in Large Scale Composites," *Heat Transfer: Korea—U.S. Seminar on Thermal Engineering and High Technology*, J. H. Kim, Sung Task Ro, and Taik Sik Lee, eds., Hemisphere, Washington, DC, pp. 55-88.

Gebhart, B., Jaluria, Y., Mahajan, R. L., and Sammakia, B., 1988, *Buoyancy Induced Flows and Transport*, Hemisphere, Washington, DC.

Kline, S. J., and McClintock, F. A., 1953, "Describing Uncertainties in Single-Sample Experiments," *Mechanical Engineering*, Vol. 75, pp. 3-8.

McAdams, W. H., 1955, *Heat Transmission*, 3rd ed., McGraw-Hill, New York.

Yang, Wen-Jei, Takizawa, H., and Vrable, D. L., 1991, "Augmented Boiling on Copper-Graphite Composite Surface," *International Journal of Heat and Mass Transfer*, in press.

Natural Convection in a Vertical Enclosure Filled With Anisotropic Porous Media

J. Ni[1] and C. Beckermann[2]

Introduction

Anisotropic porous media are encountered in numerous systems in industry and nature. Examples include fibrous materials (e.g., insulation, filters), sedimentary soils, rock formations, certain biological materials, columnar dendritic structures formed during solidification of multicomponent mixtures, and preforms of aligned ceramic or graphite fibers used in casting of metal matrix composites. Stacks of perforated plates and tube bundles (e.g., in nuclear reactor cores) may also be modeled as anisotropic porous media. Natural convection in such anisotropic porous media has received relatively little research attention. Several studies have been reported on natural convection in horizontal anisotropic porous layers heated from below (Epherre, 1977; Castinel and Combarnous, 1977; Kvernvold and Tyvand, 1979; McKibbin and Tyvand, 1982; Gjerde and Tyvand, 1984; Nilsen and Storesletten, 1990), where the permeability and/or effective thermal conductivity were taken to be different in the horizontal and vertical directions. These investigations deal mainly with the onset of convection and the flow and heat transfer phenomena at moderately supercritical Rayleigh numbers.

Castinel and Combarnous (1977) also analyzed the case of inclined layers, while Burns et al. (1977) examined natural convection in a vertical slot filled with an anisotropic porous medium. In these two studies, the porous medium was taken to be thermally isotropic. As shown by Neale (1977), this represents a good approximation for clusters of parallel fibers; however, no general conclusions can be drawn for a conducting matrix (e.g., with thin parallel copper threads introduced into the matrix) (Kvernvold and Tyvand, 1979). Furthermore, Burns et al. (1977) only studied natural convection in a relatively large aspect ratio slot and for relatively small differences in the permeabilities in the horizontal and vertical directions, which is relevant to fibrous insulation between walls in building structures. Detailed information on the flow and heat transfer phenomena in anisotropic porous media heated/cooled from the sides is presently not available.

Of related interest are the numerous studies of natural convection in porous media with layers of different permeabilities and/or effective thermal conductivities (e.g., McKibbin and O'Sullivan, 1981; Poulikakos and Bejan, 1983; McKibbin and Tyvand, 1983; Lai and Kulacki, 1988) as well as with a non-

[1]Research Assistant, Department of Mechanical Engineering, The University of Iowa, Iowa City, IA 52242.

[2]Assistant Professor, Department of Mechanical Engineering, The University of Iowa, Iowa City, IA 52242; Assoc. Mem. ASME.

Contributed by the Heat Transfer Division of THE AMERICAN SOCIETY OF MECHANICAL ENGINEERS. Manuscript received by the Heat Transfer Division February 14, 1991; revision received May 8, 1991. Keywords: Flow Nonuniformity, Natural Convection, Porous Media.

uniform porosity, for example, near the walls in packed beds of spheres (e.g., Hong et al., 1987; David et al., 1988). In general, studies of natural convection in such *heterogeneous* porous media have revealed that the flow is channeled in regions (or layers) of higher permeability, while discontinuities between layers cause sharp bends in both streamline and isotherm patterns. McKibbin and Tyvand (1982) and Gjerde and Tyvand (1984) have shown that a periodically layered porous medium can be modeled as a *homogeneous* anisotropic medium, provided the length scale of the flow is larger than the layering period. Therefore, convection phenomena such as flow channeling may be expected to be present also in the homogeneous anisotropic porous media studied here. Whereas detailed comparisons between periodically layered and homogeneous anisotropic porous media have been made for the case of heating from below (McKibbin and Tyvand, 1982; Gjerde and Tyvand, 1984), no results have been reported for the corresponding cases with heating/cooling from the sides. More recently, Angot and Caltagirone (1990) have developed a numerical method for calculating natural convection flows inside periodic heterogeneous porous structures.

The objective of the present study is to obtain an improved understanding of natural convection flow and heat transfer in a vertical enclosure filled with homogeneous porous media that are both hydrodynamically and thermally anisotropic. This fundamental study considers a two-dimensional, square enclosure with sides of length L. The left and right vertical walls are held isothermally at T_H and T_C, respectively, while the horizontal top and bottom walls are adiabatic. Relatively large ranges of the Rayleigh number (based on the permeability) and the ratios of the permeabilities and effective thermal conductivities in the horizontal and vertical directions are examined, in order to obtain a complete understanding of their influence on the flow and heat transfer processes. Results are reported in terms of streamlines, isotherms, and the overall heat transfer rates across the enclosure.

Model Equations

The flow in the square enclosure is steady, laminar, two-dimensional, and incompressible, and the thermophysical properties are assumed to be constant except for the density in the buoyancy term. The principal directions of the permeabilities (K) and (effective) thermal conductivities (k) coincide with the horizontal (x) and vertical (y) coordinate axes. Assuming the validity of Darcy's law and thermal equilibrium between the solid matrix and the fluid, the governing equations can be written in dimensionless form as

$$\frac{\partial u}{\partial \xi}+\frac{\partial v}{\partial \eta}=0 \tag{1}$$

$$0=-\frac{\partial p}{\partial \xi}-u \tag{2}$$

$$0=-\frac{\partial p}{\partial \eta}-\frac{v}{K^*}+\mathrm{Ra}\Theta \tag{3}$$

$$u\frac{\partial \Theta}{\partial \xi}+v\frac{\partial \Theta}{\partial \eta}=\frac{\partial^2 \Theta}{\partial \xi^2}+k^*\frac{\partial^2 \Theta}{\partial \eta^2} \tag{4}$$

The boundary conditions are

$$\Theta=1 \quad \text{at } \xi=0,\ 0\le\eta\le 1$$

$$\Theta=0 \quad \text{at } \xi=1,\ 0\le\eta\le 1$$

$$\frac{\partial \Theta}{\partial \eta}=0 \quad \text{at } \eta=0,\ 1,\ 0\le\xi\le 1 \tag{5}$$

$$u,\ v=0 \quad \text{on all enclosure walls.}$$

In the above equations, the coordinates (ξ, η), velocities (u, v), and pressure (p) are made dimensionless using L, α/L, and $\mu\alpha/K_x$ as the reference length, velocity, and pressure, respectively, where α is the thermal diffusivity based on k_x and μ is the dynamic viscosity. The dimensionless temperature Θ is defined as $(T-T_C)/(T_H-T_C)$. Equations (1)–(5) show that the present problem is governed by three dimensionless parameters, namely

$$\mathrm{Ra}=\frac{g\beta(T_H-T_C)K_xL}{\nu\alpha} \quad \text{Rayleigh number,}$$

$$K^*=\frac{K_y}{K_x} \quad \text{permeability ratio,} \tag{6}$$

$$k^*=\frac{k_y}{k_x} \quad \text{thermal conductivity ratio}$$

where g, β, and ν are the gravitational acceleration, coefficient of thermal expansion, and kinematic viscosity, respectively.

The overall heat transfer rate across the enclosure is expressed by the average Nusselt number at the left and right vertical walls defined as

$$\mathrm{Nu}\,|_{\xi=0,1}=\frac{\bar{h}L}{k_x}=-\int_0^1 \left.\frac{\partial \Theta}{\partial \xi}\right|_{\xi=0,1} d\eta \tag{7}$$

where $\bar{h}$ is the average convective heat transfer coefficient. Note that the Nusselt number is equal to unity in the absence of convection.

Numerical Procedures

Numerical solutions of the governing equations were obtained using the control-volume formulation described in detail by Patankar (1980). The algorithm was somewhat modified to accommodate the special form of the momentum equations and the different thermal conductivities in the ξ- and η-directions in the energy equation.

Numerical experiments were performed to establish the number and distribution of control volumes required to produce accurate results. The numerical solutions presented in this paper were acquired using 50×50 control volumes. Doubling of the number of control volumes produced essentially the same results. The distribution of the control volumes was strongly skewed toward all solid surfaces in order to resolve velocity and temperature gradients accurately. For this purpose, the grid spacing was adjusted in a trial and error fashion according to the thickness of the boundary layers. Convergence of the numerical solution was checked by performing overall mass and energy balances. The calculations were performed on an Encore minicomputer and typically required 200 CPU minutes. For the limiting case of an isotropic porous medium, a comparison of the average Nusselt numbers with those obtained in other studies is presented in Table 1. It can be seen that the present Nusselt numbers fall within 1 percent of the high-resolution finite difference calculations of Shiralkar et al. (1983). It was already noted by Walker and Homsy (1978) that their semi-analytical technique gave Nusselt numbers that are somewhat lower than previous numerical results. Good agreement was also obtained with analytical solutions for the limiting case of two-dimensional anisotropic heat conduction in a square region (Ozisik, 1980).

Table 1 Comparison of Nusselt numbers between present and previously published results ($K^*=1$, $k^*=1$, square enclosure)

Ra	Present (50×50 grid)	Walker and Homsy (1978)	Shiralkar et al. (1983)
100	3.103	3.097	3.115
500	8.892	8.66	8.944
1000	13.42	12.96	13.534

Results and Discussion

It is first instructive to examine the ranges of the governing dimensionless parameters Ra, K^*, and k^* considered in the present study. Results are presented for Rayleigh numbers of 100, 500, and 1000. Preliminary computational runs indicated that the trends for the Nusselt numbers are similar for somewhat lower and higher Rayleigh numbers. The permeability and conductivity ratios were varied (independently) from 0.001 to 1000. Whereas permeability ratios of more than 100 have been observed, for example, in sedimentary rocks (Davis, 1969), very large (or small) thermal conductivity ratios are unlikely to exist in practical systems (Neale, 1977). Also, in reality the permeability and thermal conductivity ratios are often related to each other. However, the present ranges were chosen to illustrate the trends and limiting behaviors present in natural convection in anisotropic media. Consideration of such extreme values of these ratios also aids in understanding the heat and fluid flow phenomena in the present system.

Isotherms and Streamlines. Representative streamlines and isotherms are shown in Fig. 1 for Ra = 1000. Figure 1(*a*) illustrates the streamlines and isotherms for the isotropic case (i.e., $K^* = k^* = 1$). A clockwise rotating convection cell exists in the enclosure with thermal and velocity boundary layers at the isothermal left and right walls. The isotherms outside the thermal boundary layers are almost horizontal and equally spaced, indicating that the heat transfer is by conduction between the horizontally flowing fluid streams through the relatively stagnant core.

Figure 1(*b*) shows the streamlines and isotherms for $K^* = 1000$ and $k^* = 1$. For $K^* = 1000$, the permeability in the η direction is much greater than the permeability in the ξ direction. Consequently, the buoyancy-induced flow along the vertical isothermal wall is much stronger than for $K^* = 1$. Interestingly, the flow is channeled along the vertical walls, such that the velocity boundary layer is very thin. This occurs even though the porous medium is homogeneous. The channeling effect can be attributed to the fact that the relatively low permeability in the ξ direction prevents the vertical boundary layer from thickening. The fluid attains the hot (cold) wall temperature within a short distance from the bottom (top) of the left (right) wall, and uniformly spreads over the remaining length of the wall into the horizontal direction. The isotherms form a diagonal band extending from the lower left to the upper right corner, while the upper left and lower right triangles on either side of the diagonal are virtually isothermal and at the hot and cold wall temperatures, respectively. The diagonal band of isotherms can be directly attributed to the flow patterns described above and indicates strong heat exchange between the hot and cold fluid flowing on either side.

The opposite extreme is shown in Fig. 1(*c*). For $K^* = 0.001$ (and $k^* = 1$), no velocity (or thermal) boundary layers exist along the vertical walls, while the horizontally flowing fluid is strongly channeled along the upper and lower adiabatic walls. Due to the relatively low permeability in the η direction, the natural convection flow is very weak when compared to $K^* = 1$. Consequently, the isotherms are almost vertical and equally spaced, indicating that the heat transfer across the enclosure is mostly by conduction. The low permeability in the η direction also causes the flow outside the "horizontal channels" to be completely parallel to the vertical walls and evenly spread over the left and right halves of the enclosure. In other words, the relatively high permeability in the ξ direction effectively prevents any nonuniformities from forming in the velocity profile of the vertically flowing fluid. Once the fluid reaches the upper or lower walls, it bends sharply and merges into the fast flowing fluid in the horizontal channels. Again, this channeling occurs, even though the porous medium is homogeneous.

Figures 1(*d*) and 1(*e*) show the streamlines and isotherms for different thermal conductivity ratios and $K^* = 1$. For

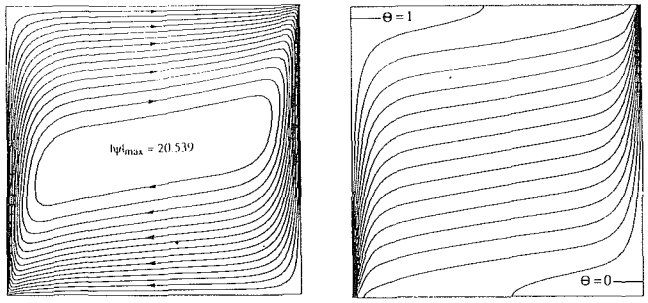

Fig. 1(*a*) $K^* = 1$, $k^* = 1$

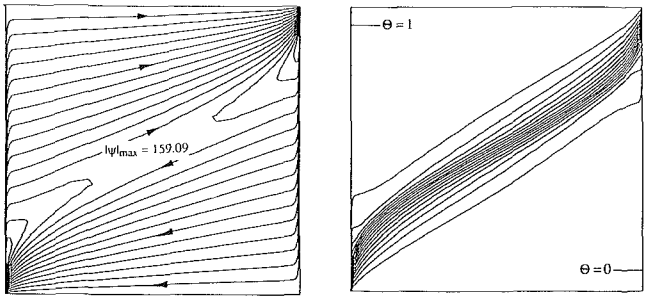

Fig. 1(*b*) $K^* = 1000$, $k^* = 1$

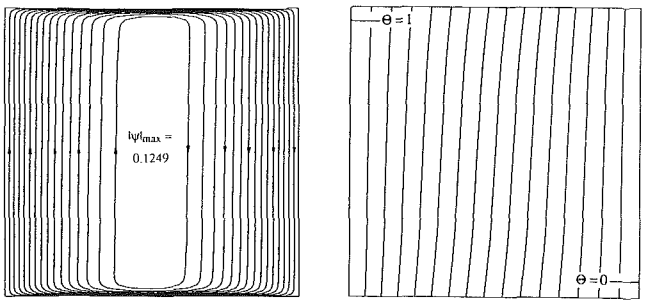

Fig. 1(*c*) $K^* = 0.001$, $k^* = 1$

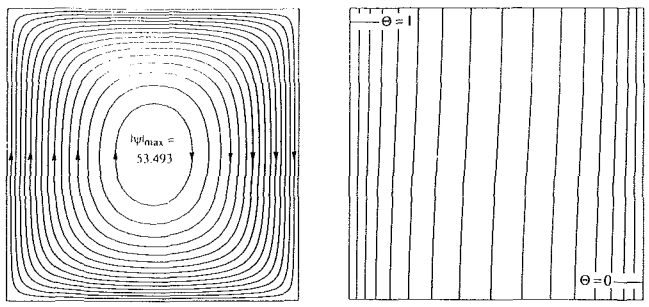

Fig. 1(*d*) $K^* = 1$, $k^* = 1000$

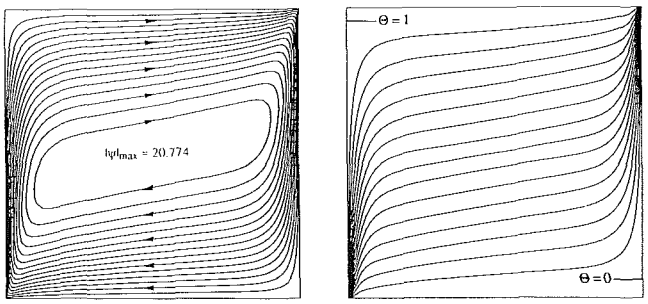

Fig. 1(*e*) $K^* = 1$, $k^* = 0.001$

Fig. 1 Streamlines (left) and isotherms (right) for Ra = 1000 (equal increments)

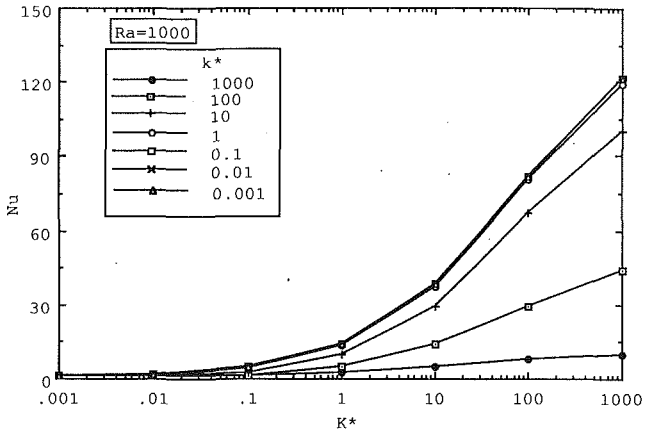

Fig. 2 Effect of permeability and thermal conductivity ratios on Nusselt number for Ra = 1000

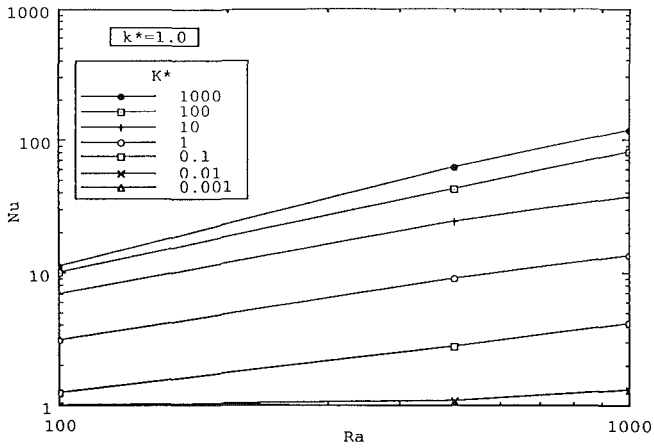

Fig. 3(*a*) $k^* = 1$ and various permeability ratios

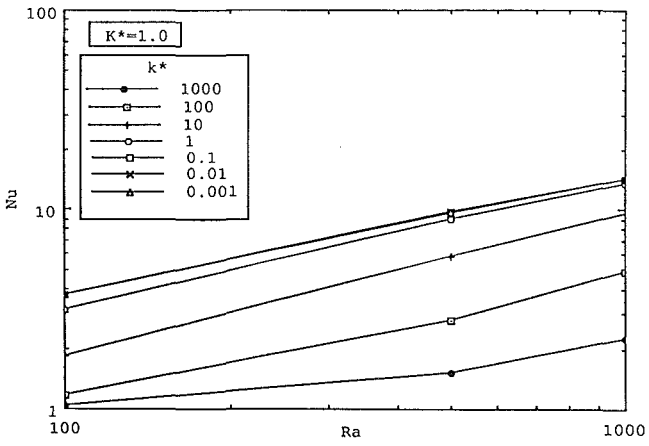

Fig. 3(*b*) $K^* = 1$ and various thermal conductivity ratios

Fig. 3 Nusselt number as a function of Rayleigh number

$k^* = 1000$ (Fig. 1*d*), the thermal conductivity is much higher in the η direction than in the ξ direction. Due to the relatively high thermal conductivity in the η direction, there exist virtually no temperature gradients in the η direction and the isotherms are almost vertical. The isotherms are only slightly more concentrated near the left and right isothermal walls, indicating that the heat transfer is mostly by conduction. Consequently, the flow exhibits almost no boundary layers and is typical of natural convection at a much lower Rayleigh number. However, the flow intensity is more than 2.5 times higher than for $k^* = 1$ (Fig. 1*a*).

Interestingly, a low thermal conductivity ratio has very little influence on the flow and heat transfer patterns. The streamlines and isotherms shown in Fig. 1(*e*) for $k^* = 0.001$ are very similar to the ones for $k^* = 1$ (Fig. 1*a*). For $k^* = 0.001$, the thermal conductivity is much lower in the η direction than in the ξ direction. It can be seen that the isotherms outside the thermal boundary layers are slightly more horizontal than for $k^* = 1$, indicating the influence of the low thermal conductivity in the η direction. Because the isotherm patterns are almost identical for $k^* \doteq 0.001$ and 1, the natural convection flow for $k^* = 0.001$ is also very similar to the one for $k^* = 1$.

Nusselt Numbers. Figure 2 shows the effect of the permeability and thermal conductivity ratios on the Nusselt number for Ra = 1000. It can be seen that for all thermal conductivity ratios, the Nusselt numbers approach unity as $K^* \to 0$. As expected Nu increases with increasing K^*. For all permeability ratios, the Nusselt numbers approach unity for $k^* \to \infty$ and increase with decreasing k^*. At a given permeability ratio, the Nusselt numbers are about the same for $k^* < 1$. All of the above results are in agreement with the observations made in the previous section. One important conclusion is that K^* and k^* have generally opposing effects on Nu.

Figure 3 summarizes all numerical data for the Nusselt number obtained in the present study. In this figure, Nu is plotted as a function of Ra for various permeability (Fig. 3*a*) and thermal conductivity (Fig. 3*b*) ratios. For isotropic porous media, it has been found that the Nusselt number can be well correlated by an equation of the form $\mathrm{Nu} = c\mathrm{Ra}^n$, with the exponent n being a weak function of Ra (Shiralkar et al., 1983). Figure 3 shows that the slopes of the Nu versus Ra curves are quite similar for relatively large ranges of the permeability and thermal conductivity ratios. However, the curves are shifted considerably upward or downward (relative to $K^* = k^* = 1$) for the various permeability and thermal conductivity ratios (except for $k^* < 1$). This indicates that in the Nusselt number correlation, the exponent n of the Rayleigh number is only a weak function of K^* and k^*, while the "constant" c depends strongly on both K^* and k^* (except for $k^* < 1$). In fact, for relatively small deviations of K^* and k^* from unity (i.e., $0.1 < K^* < 10$ and $0 < k^* < 10$), correlations for Nu such as those proposed by Shiralkar et al. (1983) for an isotropic porous medium may be utilized, if the "constant" c is appropriately modified to reflect its dependence on K^* and k^*.

Conclusions

A numerical study has been performed of natural convection in a vertical enclosure containing hydrodynamically and thermally anisotropic porous media. When compared to isotropic porous media, natural convection in the anisotropic case has the following physical characteristics:

(*i*) A large permeability ratio ($K^* > 1$) caused channeling of the flow along the vertical isothermal walls, a higher flow intensity in the enclosure, and, consequently, a higher Nusselt number.

(*ii*) A low permeability ratio ($K^* < 1$) causes channeling of the flow along the horizontal boundaries, thicker velocity boundary layers along the vertical walls, a lower flow intensity in the enclosure, and, hence, a smaller Nusselt number. All Nusselt numbers approach unity in the limit of $K^* \to 0$.

(*iii*) A large thermal conductivity ratio ($k^* > 1$) causes a higher flow intensity in the enclosure, the isotherms to be more vertical, the heat transfer to be more dominated by conduction, and, hence, a lower Nusselt number. All Nusselt numbers approach unity in the limit of $k^* \to \infty$.

(*iv*) A low thermal conductivity ratio ($k^* < 1$) has very little influence on the flow and heat transfer patterns, and the Nusselt numbers for a given Ra and K^* are approximately the same as for $k^* = 1$.

(v) The permeability and thermal conductivity ratios generally have opposing effects on the Nusselt number.

(vi) The dependence of the flow and heat transfer on the Rayleigh number is quite similar to the isotropic case, while the absolute values of the Nusselt number change drastically for $K^* \neq 1$ and $k^* > 1$.

In conclusion, the present results revealed a number of interesting convection phenomena that need more research attention. It is hoped that this exploratory numerical study will stimulate further research into the important, but hitherto rather neglected, area of natural convection in both hydrodynamically and thermally anisotropic porous media. Additional work should also include investigations of inertia effects for relatively small Prandtl numbers and boundary effects for large Darcy numbers (i.e., permeabilities). The latter effect could be particularly important in the present system, due to the strong flow channeling observed along the solid boundaries.

Acknowledgments

The work reported in this paper was supported, in part, by the National Science Foundation under Grant No. CBT-8808888. Computer facilities were made available by The University of Iowa WEEG Computing Center.

References

Angot, Ph., and Caltagirone, J. P., 1990, "Natural Convection Through Periodic Porous Media," in: *Heat Transfer 1990*, G. Hetsroni, ed., Hemisphere, New York, Vol. 5, pp. 219–224.

Burns, P. J., Chow, L. C., and Tien, C. L., 1977, "Convection in a Vertical Slot Filled With Porous Insulation," *Int. J. Heat Mass Transfer*, Vol. 20, pp. 919–926.

Castinel, G., and Combarnous, M., 1977, "Natural Convection in an Anisotropic Porous Layer," *Int. Chemical Eng.*, Vol. 17, pp. 605–614.

David, E., Lauriat, G., and Cheng, P., 1988, "Natural Convection in Rectangular Cavities Filled With Variable Porosity Media," in: *ASME Proceedings of the 1988 National Heat Transfer Conference*, H. R. Jacobs, ed., ASME, New York, Vol. 1, pp. 605–612.

Davis, S. N., 1969, "Porosity and Permeability of Natural Materials," in: *Flow Through Porous Media*, J. M. De Wiest, ed., Academic Press, New York, pp. 53–89.

Epherre, J. F., 1977, "Criterion for the Appearance of Natural Convection in an Anisotropic Layer," *Int. Chemical Eng.*, Vol. 17, pp. 615–616.

Gjerde, K. M., and Tyvand, P. A., 1984, "Thermal Convection in a Porous Medium With Continuous Periodic Stratification," *Int. J. Heat Mass Transfer*, Vol. 27, pp. 2289–2295.

Hong, J. T., Yamada, Y., and Tien, C. L., 1987, "Effects of Non-Darcian and Nonuniform Porosity on Vertical Plate Natural Convection in Porous Media," ASME JOURNAL OF HEAT TRANSFER, Vol. 109, pp. 356–362.

Kvernyold, O., and Tyvand, P. A., 1979, "Nonlinear Thermal Convection in Anisotropic Porous Media," *J. Fluid Mechanics*, Vol. 90, pp. 609–624.

Lai, F. C., and Kulacki, F. A., 1988, "Natural Convection Across a Vertical Layered Porous Cavity," *Int. J. Heat Mass Transfer*, Vol. 31, pp. 1247–1260.

McKibbin, R., and O'Sullivan, M. J., 1981, "Heat Transfer in a Layered Porous Medium Heated From Below," *J. Fluid Mechanics*, Vol. 111, pp. 141–173.

McKibbin, R., and Tyvand, P. A., 1982, "Anisotropic Modelling of Thermal Convection in Multilayered Porous Media," *J. Fluid Mechanics*, Vol. 118, pp. 315–339.

McKibbin, R., and Tyvand, P. A., 1983, "Thermal Convection in a Porous Medium Composed of Alternating Thick and Thin Layers," *Int. J. Heat Mass Transfer*, Vol. 26, pp. 761–780.

Neale, G., 1977, "Degrees of Anisotropy for Fluid Flow and Diffusion Through Anisotropic Porous Media," *AIChE Journal*, Vol. 23, pp. 56–62.

Nilsen, T., and Storesletten, L., 1990, "An Analytical Study on Natural Convection in Isotropic and Anisotropic Porous Channels," ASME JOURNAL OF HEAT TRANSFER, Vol. 112, pp. 396–401.

Ozisik, M. N., 1980, *Heat Conduction*, Wiley, New York.

Patankar, S. V., 1980, *Numerical Heat Transfer and Fluid Flow*, McGraw-Hill, New York.

Poulikakos, D., and Bejan, A., 1983, "Natural Convection in Vertically and Horizontally Layered Porous Media Heated From the Side," *Int. J. Heat Mass Transfer*, Vol. 26, pp. 1805–1814.

Shiralkar, G. S., Haajizadeh, M., and Tien, C. L., 1983, "Numerical Study of High Rayleigh Number Convection in a Vertical Porous Enclosure," *Numerical Heat Transfer*, Vol. 6, pp. 223–234.

Walker, K. L., and Homsy, G. M., 1978, "Convection in a Porous Cavity," *J. Fluid Mechanics*, Vol. 87, pp. 449–474.

Analysis of Heat Flux Measurement by Circular Foil Gages in a Mixed Convection/Radiation Environment

C. H. Kuo[1,3] and A. K. Kulkarni[2,3]

Nomenclature

h = convective heat transfer coefficient

$I_o(r)$, $I_1(r)$ = Bessel's functions of the first kind

k = thermal conductivity of the circular foil

m = $\sqrt{h/k\delta}$

q_c = convective heat flux per unit area to the surface (or wall)

q_g = gage-sensed heat flux per unit area

q_m = mixed (radiative and convective) heat flux per unit area to the surface (or wall) when $T_w = T_B$

q_r = total heat flux per unit area to the surface (or wall) obtained from the gage output using radiation-based calibration

q'_r = radiative heat flux per unit area absorbed by the gage

q_w = total (mixed) heat flux per unit area to the surface when $T_w \neq T_B$

r = radial coordinate of circular foil

R = radius of the circular foil

$T(r)$ = temperature distribution in circular foil

T_o = temperature at the foil center

T_B = temperature of heat sink (base), which is maintained constant

T_w = surface (wall) temperature

T_∞ = temperature of gas flowing over the surface

δ = thickness of foil

ΔT_r, ΔT_c, ΔT_m = temperature difference between the foil center and edge with pure radiation heat flux, pure convection heat flux, and mixed convection/radiation heat flux, respectively

Introduction

Principles of heat flux measurement by circular foil heat flux sensors, also known as Gardon gages, are analyzed when the gages are subjected to a mixed convective/radiative heat flux. A schematic of the Gardon gage is shown in Fig. 1. The gage is constructed using a copper cylinder (usually water-cooled) with a thin constantan foil mounted on the top. A copper wire is welded at the foil center and the copper cylinder is used as the other conductor, creating a differential thermocouple between the center and the edge of the foil. The gage is mounted flush on a surface at a location where a measurement of total heat flux to the surface is desired. The heat flux incident on the constantan foil of the gage causes a temperature difference, ΔT, between the foil center and the edge, which generates a corresponding voltage signal. Measurement of ΔT is then converted into the total incident heat flux using a calibration curve or chart. Calibration is usually

[1]Graduate Student.

[2]Associate Professor.

[3]Department of Mechanical Engineering, The Pennsylvania State University, University Park, PA 16802.

Contributed by the Heat Transfer Division and presented at the ASME/JSME Joint Heat Transfer Conference, Reno, Nevada, March 1991. Manuscript received by the Heat Transfer Division June 23, 1990; revision received February 15, 1991. Keywords: Conjugate Heat Transfer, Instrumentation, Measurement Techniques.